A new approach to relay-based autotuning PID controllers and their evaluation in pH control of industrial photobioreactors

Caparroz, Malena; Soltesz, Kristian; Hägglund, Tore; Guzmán, José Luis; Berenguel, Manuel

Published in:
Control Engineering Practice

DOI:
10.1016/j.conengprac.2025.106520

2025

Document Version:
Peer reviewed version (aka post-print)

A new approach to relay-based autotuning PID controllers and their evaluation in pH control of industrial photobioreactors

Malena Caparroz[a], Kristian Soltesz[b], Tore Hägglund[b], José Luis Guzmán[a], Manuel Berenguel[a]

[a] *University of Almería, Department of Informatics, ceiA3, CIESOL, Ctra. Sacramento s/n, Almería, 04120, Spain*
[b] *Lund University, Department of Automatic Control, Box 118, Lund, SE-221 00, Sweden*

Abstract

This paper presents a novel adaptive autotuning strategy for controlling the pH in microalgae raceway reactors, a critical variable in optimizing biomass productivity under dynamic environmental conditions. The method expands on existing relay-based autotuning principles, tailored to suit the seasonally variable dynamics of microalgae cultivation systems influenced by CO_2 injection and photosynthetic activity. The novelty of the proposed approach relies on the use of a relay-based autotuning technique that applies the relay signal to the setpoint and not to the control signal. This method allows for seamless integration into existing control loops without manual recalibration across seasons. Moreover, the method is coupled with a classification algorithm to assess weather conditions, enhancing the reliability of autotuning under fluctuating solar radiation. Using the developed autotuning method, low-order models are identified, and the autotuner is coupled with a Proportional-Integral controller plus a static feedforward compensation to counteract solar radiation disturbances. The designed algorithm has been successfully evaluated for five consecutive days in a real semi-industrial-scale raceway reactor and compared with a classical PI with a feedforward strategy. The results demonstrate reliable performance across clear and cloudy conditions, offering a scalable and automated solution for adaptive pH regulation in microalgae production systems.

Keywords: Autotuning, Process control, pH regulation, Microalgae production

1. Introduction

In recent decades, microalgae have garnered increasing attention for their potential to address critical challenges related to climate change. Their applications span diverse sectors, including food, energy, wastewater treatment, and carbon dioxide fixation [1, 2]. Microalgae offer a sustainable solution, as they do not compete with food crops for arable land, exhibit high oil content suitable for biofuel production, can be cultivated in various aqueous media (including wastewater), generate oxygen, and effectively capture CO_2 [3].

However, the large-scale cultivation of microalgae presents several control challenges. Efficient microalgae production relies on precisely regulating key culture variables within the cultivation system. These variables include pH, dissolved oxygen, culture temperature, and nutrient levels [2, 4, 5].

Among these, pH is particularly critical, as it profoundly influences the growth, metabolism, and availability of essential nutrients in the microorganisms. In [6] and [7], it was proven that a lack of pH control leads to significantly less favourable conditions. Uncontrolled pH results in a decrease in inorganic carbon availability, leading to minimal biomass productivity. Keeping pH under control is essential to avoid carbon limitation and increase productivity. In addition to directly impacting carbon metabolism and productivity, pH control is crucial to ensure a stable culture, reducing the risk of system collapse and cell death due to disturbances. It also influences the microbial community, promoting the growth of the desired algal strain, reducing contamination by fungal predators and rotifers, impacting the activity of nitrifying bacteria, and enhancing the elimination of pathogens through synergy with solar radiation and temperature. Therefore, implementing pH control strategies is indispensable to overcoming the limitations of open raceway systems and improving the efficiency

Email addresses: mcaparroz@ual.es (Malena Caparroz), kristian@control.lth.se (Kristian Soltesz), tore.hagglund@control.lth.se (Tore Hägglund), joguzman@ual.es (José Luis Guzmán), beren@ual.es (Manuel Berenguel)

and sustainability of large-scale microalgae production.

This variable is characterized by having complex dynamics that can have significant variations. These changes can arise from diurnal cycles, seasonal changes, and fluctuations in culture conditions such as biomass concentration and culture state. For instance, the rate of photosynthesis, and consequently the rate of pH increase, varies significantly throughout the day, with higher rates observed during periods of intense solar radiation. Similarly, seasonal changes in solar irradiance and temperature can alter the overall metabolic activity of the microalgae culture, impacting both the consumption of CO_2 and the efficiency of CO_2 injection for controlling pH. These factors contribute to the time-varying nature of the system's dynamics, making it challenging to maintain optimal conditions [8]. Therefore, a key challenge in controlling microalgae cultivation systems is obtaining accurate and reliable models, but the inherent complexity and variability of biological processes hinder this identification.

In the last decades, several efforts have been made in the scientific community to obtain these models [9, 10]. This has resulted in a wide variety of descriptions, with different complexities, advantages, and disadvantages. The simplest models that can be found are linear models, as developed in [9], which relate the pH with the CO_2 injection and the solar radiation through low-order transfer functions. However, they frequently fail to capture the full complexity of the system dynamics, particularly in the presence of nonlinearities and time-varying parameters. Consequently, controllers designed based on these models may exhibit suboptimal performance under changing operating conditions. Furthermore, in [11], it is shown that the parameters of these simple models strongly depend on the culture conditions. Other types of models that can be found in the literature are data-based ones, with more complex structures. They can consist of machine or deep learning techniques, such as the artificial neural networks developed in [12]. These types of models require a large amount of data with a wide variety of conditions in order to obtain an accurate description of the system. Lastly, first-principles-based models like the one developed in [10] are the most accurate, allow a deep comprehension of the system, and are very suitable for process optimization and development of simulators. However, they include several parameters whose values are hard to estimate accurately and can make the design of controllers difficult.

The limitations of these types of models highlight the need for control strategies that can effectively handle the inherent uncertainties and time-varying dynamics of microalgae cultivation systems. Adaptive control techniques offer a promising solution to this challenge. Unlike traditional control methods with fixed parameters, adaptive controllers can maintain performance even when the system's behaviour changes over time [13]. This is particularly advantageous in microalgae cultivation, where environmental conditions, culture characteristics, and system parameters vary significantly. In previous works, adaptive control techniques were developed for this problem. In [11], an adaptive control algorithm based on regression-tree models was developed for pH, where the controller parameters were adapted based on the weather and reactor conditions. In [14], a hybrid MRAC algorithm was instead tested in a raceway reactor to demonstrate how the performance could be improved by adapting the setpoint to the control loop. Although those solutions demonstrated that adaptive control approaches can highly contribute to improving the performance of the pH control, they presented significant limitations with respect to the need of a large dataset to train the model in the case of [11], or the sensitivity of the tuning parameters in the MRAC algorithm in [14].

Another approach to adaptive control involves the use of autotuners, which can contribute to reducing the limitations of the already tested solutions mentioned above. An autotuner is an algorithm that automatically tunes the parameters of a controller. Traditional methods for tuning controllers often rely on manual adjustments or offline experiments, which can be time-consuming and require specialized expertise. Autotuners, on the other hand, automate the tuning process, reducing the need for manual intervention and improving the efficiency of controller implementation. The relay autotuner methodology, first introduced in [15], is a well-established technique for automatically tuning controllers. It involves introducing a relay feedback into the control loop, which induces oscillations in the system output. By analyzing these oscillations, the autotuner can estimate key parameters of the system dynamics, such as the static gain and time constant, and use this information to tune the controller parameters.

In this work, two different autotuning control strategies are studied: the first one is the classical approach, in which the controller is disconnected when the identification experiment is performed, and the relay signal is directly applied to the control signal. The second strategy introduces a novel approach to this technique by applying the relay signal to the setpoint and maintaining the controller working during the experiment. Notice that this approach allows a better management of initially unknown model parameters and reduces sensi-

tivity with respect to disturbance effects. Both methods were implemented in the real facilities and, while proving in both cases a proper excitation of the system, the novel approach presented advantages over the classical procedure. Maintaining the controller plugged in allows a straightforward extrapolation of the method to facilities with different configurations, can properly excite the system during a wider variety of conditions, and dampens the oscillations in pH measurement, allowing a better model fit.

Moreover, the control strategy designed in this work includes a proportional-integral (PI) controller with a static feedforward to compensate for part of the solar radiation's effect on pH. Unlike previous works [11], where only the PI controller parameters are adapted, this work also suggests a simple adaptation for the feedforward gain, obtaining an enhanced performance of the autotuning method.

The controller was designed and implemented in a real, semi-industrial-scale raceway reactor, demonstrating a reliable algorithm for retuning the controller's parameters without requiring expert intervention.

2. Materials and methods

2.1. Facilities

During the development of this work, two raceway reactors located at the IFAPA (Andalusian Institute for Agricultural, Fisheries, Food and Organic Production Research and Training) research center, next to the University of Almería, Spain, were used (see Figure 1). Both reactors are built the same, and are located next to each other to ensure the same environmental conditions. They consist of two channels, each measuring 40 meters in length and 1 meter in width, connected by a U-shaped bend, resulting in a total area of 80 square meters. While their maximum depth is 30 centimeters, studies suggest optimal production is obtained when working at a depth of 15 centimeters [16].

Three different components can be distinguished in raceway reactors: (i) a paddlewheel that mixes and impulses the culture along the channels, (ii) a sump right after the paddlewheel, where CO_2 and air injection take place to regulate pH and dissolved oxygen, and (iii) the channels through which microalgae circulate while absorbing sunlight and performing photosynthesis.

The system is fully equipped with sensors and operates autonomously. With a sample time of 1 second, every variable involved in the process (pH, dissolved oxygen, culture temperature, etc.) and weather conditions (solar radiation, ambient temperature, relative humidity, etc.) are recorded.

Figure 1: Raceway reactors located at the IFAPA research center.

The studied strain is *Scenedesmus*, which is well adapted to the environmental conditions found in Southern Spain. It exhibits rapid growth and can thrive across a diverse range of temperature and pH levels [6, 17]. Cultivation of microalgae is done in freshwater, with nutrients being supplemented throughout the dilution process.

2.2. pH control problem

The pH is mainly influenced by CO_2 injection and solar radiation, with their effects being opposite. Upon injecting CO_2, pH starts decreasing. However, this effect is not noticed on the variable's measurement until a characteristic delay has elapsed. This time delay is caused by the distance between the sump where the CO_2 is injected and the sensor where the pH is measured, located at the end of the channel. Conversely, cessation of CO_2 injection allows the photosynthesis of microalgae to raise the pH [18]. Both dynamics are significantly influenced by environmental factors like sunlight, temperature, and culture conditions, including biomass concentration and culture depth.

These dynamics can be easily distinguished in Figure 2, where an on/off controller with hysteresis is implemented to control pH with CO_2 injection. The first subplot shows the measured pH in blue, and the setpoint and hysteresis values in a dashed line. The second and third subplots show the CO_2 flow injection, in L/min, and the PAR radiation, in $W/^2$, respectively. It can be observed that pH starts surging as soon as photosynthetically active radiation (PAR) is available. Once its value has exceeded the value of the upper hysteresis (8.3), CO_2 is injected into the reactor. The pH continues to grow until the time delay (5 minutes) has passed,

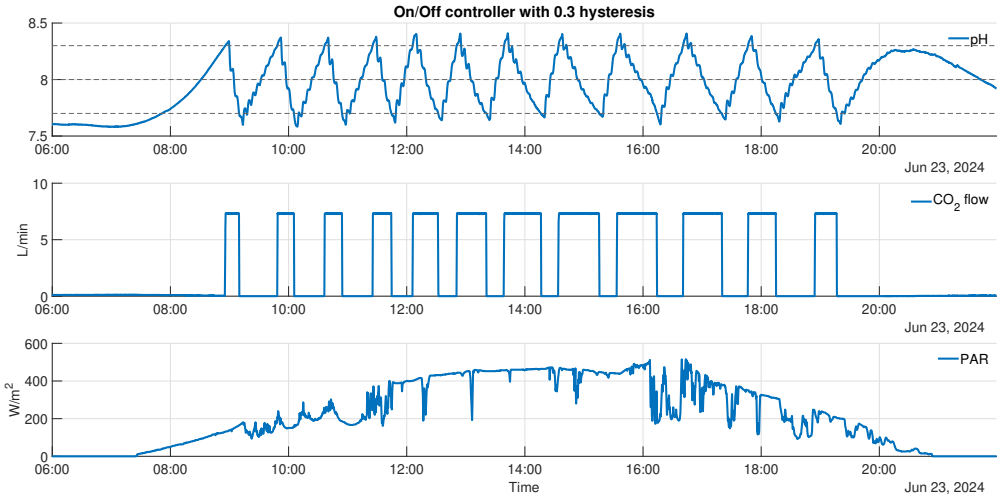

Figure 2: pH on/off controller with hysteresis. The first subplot shows the measured pH in blue, and the setpoint and hysteresis values in a dashed line. The second and third subplots show the CO_2 flow injection and the PAR radiation, respectively. A great variation in the pH's dynamic response can be observed throughout the day.

when it starts declining. Gas injection is held until the inferior hysteresis (7.7) is reached, at which instant it ceases. Once again, after the time delay has elapsed, the pH reaches a minimum and starts increasing thanks to the photosynthetic activity performed by microalgae.

It can also be noticed that the slope of the pH curve varies significantly throughout the day. It becomes clear that in the middle of the day, when solar radiation is higher, and so is photosynthetic activity, it takes longer to drop pH than in the first and last hours. On the other hand, pH rises gently when irradiance is lower, and it increases rapidly when irradiance is higher.

Another strong disturbance on pH is the dilution rate. This reflects the medium added to the reactor, and it can be done for two different reasons. The first one is the daily harvesting, which consists of extracting a certain amount of culture from the reactor to post-process it and obtain the final product. Then, the same volume of culture taken from the reactor must be replaced with water and nutrients. The other reason to dilute the reactor is for evaporation compensation. Depending on factors such as temperature, humidity, and wind, water is evaporated from the reactor during the whole day. Therefore, water is added to the reactor when the level has dropped below a specific value to maintain the culture level at its optimum. Depending on the application, the medium added during the dilution can be freshwater with chemical fertilizers, greenhouse effluents, or wastewater. The origin of the water will cause it to have a different pH in each case, which may differ from the pH at which the reactor operates, resulting in a possibly strong disturbance. In the case of this work, the dilution is made with freshwater with added fertilizers, provoking a drop in pH when added to the reactor.

Lastly, continuous fluctuations can be appreciated during the whole experiment. These are due to the recirculation of the culture along the raceway, and their period is equal to the time delay. However, these are not relevant from a modeling and control point of view since their impact on productivity is negligible.

Around the operating point, the influence of CO_2 flow injection on pH measurement can be modeled with a first-order plus time delay (FOTD) transfer function, described by equation (1),

$$G(s) = \frac{pH(s)}{CO_2(s)} = \frac{k}{\tau s + 1} \cdot e^{-t_d s}, \tag{1}$$

where pH is measured with the sensor located at the end of the channel, CO_2 is flow in L/min, s is the Laplace domain variable, k is the static gain in min/L, τ is the time constant in s and t_d is the characteristic time delay also in s. The time delay is a fixed parameter, given that the paddlewheel rotates at a constant rotational speed, fixing the speed at which the culture moves along the channel. However, the static gain and the time constant strongly depend on the conditions to which the culture is subjected [11]. These parameter variations occur during the day and fundamentally vary between the different seasons of the year. Typically, faster dynamics are observed in spring and summer, when higher values of solar radiation are obtained. However, strong variability can also be observed in different seasons based

on the biomass concentration, passing clouds, culture depth, and others. This hinders the development of a simple model that accurately describes the system's dynamics throughout the year, and promotes the development of adaptive models that can change their parameters according to the current dynamics. This work proposes an autotuner methodology to obtain a simple model whose parameters vary daily if the conditions are different enough to alter the model.

2.3. Autotuner methodology

The relay autotuner methodology was first introduced in the 1980s in [15], and some industrial applications of the technique can be found in the following years [19, 20]. However, it was not until the last decade that this approach was studied again, and some adaptations and improvements of the method were suggested [21]. The method provides a simple way of finding PID controller parameters for a process with unknown dynamics. The auto-tuning test is done under closed-loop control, ensuring the process is kept close to the setpoint. This maintains the process within a linear range where the dynamic of the response is of interest, which is why this method is effective for highly nonlinear processes [22]. The identification experiment is also characterized for its briefness, which is optimal to avoid the apparition of disturbances, which can strongly change the controlled variable dynamics and affect the identification negatively.

The first step is designing the experiment, where the type of experiment and the parameters to be used must be decided [21]. The experiment usually consists of a nonlinear function that can be described as a relay with hysteresis, and causes the process to oscillate with a small and controlled amplitude [23]. The first relay-based model identification methods were based on the following steps. When an operator decided to tune the controller, the PID was replaced with the relay function. Once the experiment was finished, the PID controller parameters were tuned, and the system switched back to PID control [15]. The experiment aimed to find the critical gain and critical period systematically and automatically [24].

Although there are several guidelines for developing an autotuner, the experiments from this work were designed considering the specific dynamics of the studied system, and previous knowledge of it was taken advantage of. Moreover, two relay-based autotuner approaches were tried, explained in detail in Section 3, introducing a novel approach in which the relay signal is applied to the setpoint and the PI controller stays plugged in during the experiment.

3. Algorithm design

3.1. Experiment design

The initial stage of the experiment design aims to determine the viability of the experiments to identify models that correctly represent the dynamics of the pH concerning the CO_2. Two options were studied for the experiment: the first one uses the original autotuner approach, by disconnecting the PI controller when the identification needs to be done (explained in Section 3.1.1). In contrast, the second one maintains the controller running and makes relay changes in the setpoint (explained in Section 3.1.2). Both options were implemented in the raceway reactors described in Section 2.1 over several days, and their parameters were tuned to obtain a sufficient excitation of the pH when performing the experiment.

In both cases, the pH was maintained at a fixed setpoint with a PI controller, and, at 1.00 p.m., the identification experiment was performed. The reason for implementing the experiment around noon is that solar radiation is at its maximum, and photosynthesis is at its highest. Therefore, pH rises faster when CO_2 flow is drastically lowered. On the contrary, if the experiments were performed during the first or last hours of the day, solar radiation would have too little effect on photosynthesis, provoking a quick drop in pH when CO_2 flow is increased, but a too slow rise when it is reduced. This would eliminate the possibility of having several switches in the behaviour in a short period.

Another essential characteristic of the implemented experiments is their hybrid nature. This means that two time-related conditions are imposed apart from the desired output hysteresis imposed in the relay experiment, which is characteristic of the classic relay autotuners. The time-related additional conditions are the following:

- The relay must remain in the same position for at least 5 minutes. The objective of this condition is to avoid a switch before the time delay has elapsed since the last change in the relay. This can otherwise be provoked by the measurement noise or the pH oscillations produced by the culture recirculation along the channel.

- The relay can stay at the same position for a maximum of 12 minutes. If solar radiation is too weak, photosynthetic activity may be low, and pH may take too long to rise to the established hysteresis. With this time limit, a minimum of three switches can be obtained during the 45 minutes of the experiment.

The timed-relay behaviour can be observed in the scheme shown in Figure 3, where the horizontal axis represents the error (e) between the setpoint (equal to 8) and the measured pH and the coordinate axis represents the amplitude of the output signal of the relay (x). The relay initially switches when the error e reaches 0.2, but this value can be increased if this error is reached before the minimum time has elapsed (T_{min} = 5 min) or it can be decreased if the maximum time has passed (T_{max} = 12 min) but the 0.2 error has not been achieved. On the other hand, the output of the relay will depend on the experiment performed. In the case of the classic approach (explained in detail in Section 3.1.1), the output will be CO_2 flow. However, when the relay is applied to the setpoint (see Section 3.1.2), the output of the relay means a change in the pH setpoint.

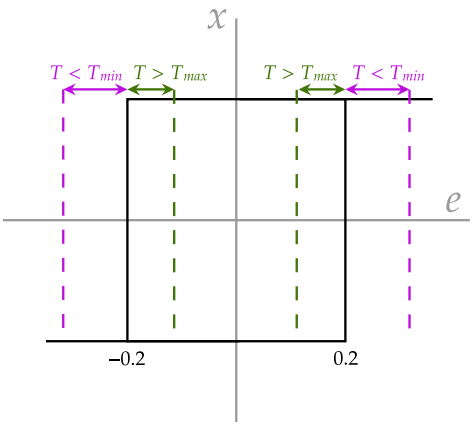

Figure 3: Timed-relay diagram. The ordinate axis (x) represents the amplitude of the output signal, and the abscissa axis (e) represents the error between the setpoint and the measured pH. This error provokes the relay switch originally when it reaches 0.2, but this value may be modified depending on the elapsed time.

It must also be mentioned that the PI controller in both cases is tuned using the SIMC rules [25], and incorporates a static feedforward gain to reject the solar radiation effect. The tuning method is detailed in Section 3.4. Finally, it is important to point out that the dilution pulses were anulled during the performance of the experiment and this operation turned back to normal once it was finished.

3.1.1. Classic relay-based experiment

In this first experiment, the classical approach was implemented. The PI controller is disconnected when the experiment is to be performed, and it is connected back after the experiment is finished, as shown in Figure 4.

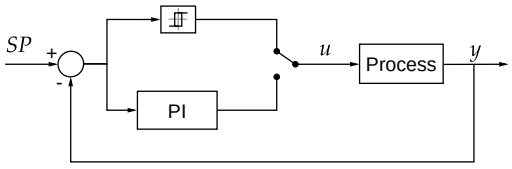

Figure 4: Classic relay-based autotuner setup, where the PI controller is disconnected when the experiment is to be performed.

In this case, the experiment consists of switching between an u_{on} and a u_{off} control signal that will provoke changes in the dynamics of the measured output. In this experimental setup, when the experiment starts, the last value of CO_2 flow in the operating point is saved (u_{op}). The on and off control signals from the experiment are calculated as $u_{on} = u_{op} + x$ and $u_{off} = u_{op} - x$, respectively, where x = 2 L/min is the amplitude of the relay, as shown in Figure 3. The amplitude of the relay applied to the control signal is fixed, and its mean value is equal to the operating point, to ensure the pH is maintained as close to its optimal value given by the setpoint (SP) as possible.

Two examples of implementing this experiment can be seen in Figures 5 and 6. The first plot shows the pH and its setpoint, set at 8. The second and third plots show the CO_2 flow in L/min and the PAR in W/m^2, respectively. In both cases, the pH is maintained on its setpoint before starting the experiment with a PI controller, ensuring that, when the experiment begins, the system is at the operating point. During the experiment period, highlighted in light pink, the CO_2 flow presents a pulse train shape, switching between u_{on} and u_{off}, allowing the pH excitation. It should also be noticed that, apart from the desired oscillations, the fluctuations produced by culture recirculation are also present. These are characterized for presenting a shorter period (5 minutes, as explained in Section 2.2), and a smaller amplitude.

Results shown in Figure 5 correspond to a clear-sky day, where PAR during the experiment is almost constant at around 240 W/m^2, while results shown in Figure 6 present strong passing clouds during the course of the experiment. This is observed in the PAR profile, which presents several abrupt drops and surges during the central hours of the day. This behaviour is typical of passing clouds and is undesirable during the identification experiment, given that it can severely affect the parameters and therefore the goodness of the obtained model.

As seen in both Figures, the experiment can excite the system properly. However, the value of x was established by trial and error. While properly exciting the

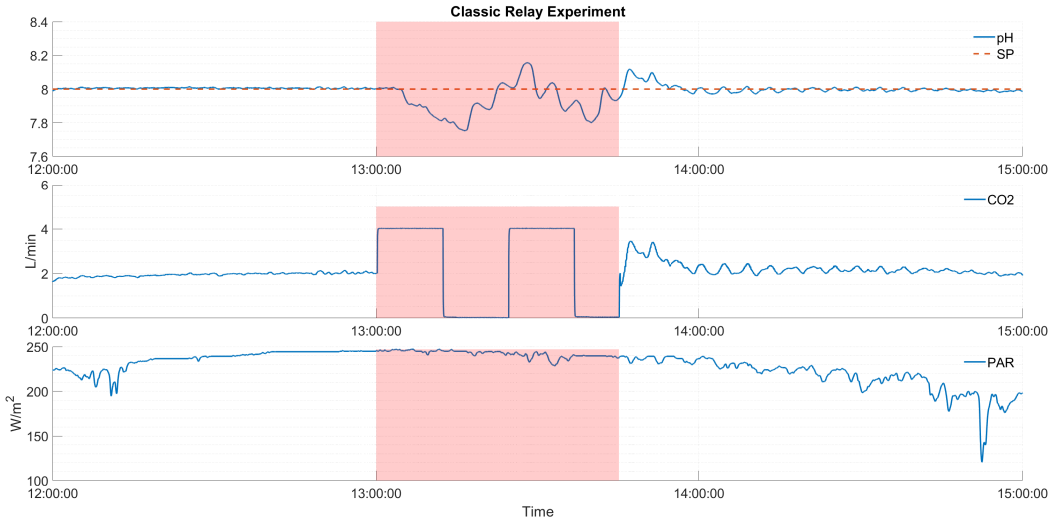

Figure 5: Classic relay-based autotuner results - Clear-sky day. The first subplot shows the pH response in blue and its setpoint in a red dashed line. The second and first subplots show the CO_2 flow and the PAR radiation, respectively. The area highlighted in pink represents the experiment duration.

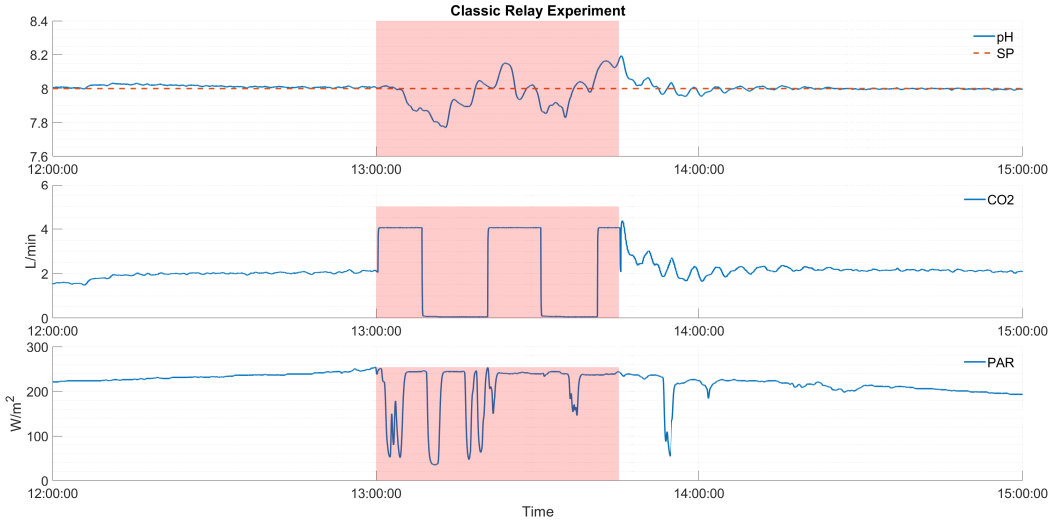

Figure 6: Classic relay-based autotuner results - Cloudy day. The first subplot shows the pH response in blue and its setpoint in a red dashed line. The second and first subplots show the CO_2 flow and the PAR radiation, respectively. The area highlighted in pink represents the experiment duration.

pH during the winter season, it could not be enough to provoke these changes during summer, where photosynthetic activity is much higher, thanks to higher solar radiation. Moreover, this amplitude value is adequate for the specific characteristics of the used reactor. If this experiment were implemented in a reactor of a different surface or configuration, this amplitude would not work with the same efficiency. Therefore, this type of experiment must be recalibrated as the climatic conditions change. This encourages the implementation of a setpoint relay-based experiment, as described in Section 3.1.2, which needs no adaptation between seasons or reactors with different dimensions.

3.1.2. Setpoint relay-based experiment

In the second identification experiment, a PI controller is fixed, and the relay signal is applied to the setpoint signal, as shown in the scheme in Figure 7. Therefore, the PI controller will be in charge of changing the CO_2 flow in order to achieve the specified amplitude on

the pH measurement. The amplitude established for the relay is $x = 0.2$, and the direction of the first change made to the setpoint depends on the sign of the error. This means that, if when the experiment is about to start, $pH > SP$, then the first setpoint of the experiment will be $SP_{relay} = SP - x$. Otherwise, if the pH is smaller than the setpoint ($pH < SP$), then the setpoint will grow ($SP_{relay} = SP + x$). As it can bee seen, when the excitation signal is introduced, a first change in the CO_2 flow is performed, due to the proportional gain, and afterwards, the integral action of the controller starts affecting the control signal.

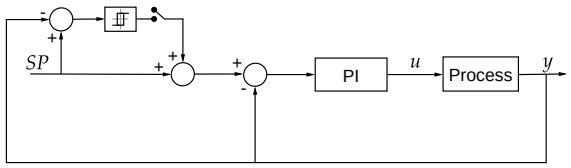

Figure 7: Setpoint relay-based autotuner setup. The relay signal is applied to the setpoint, and the PI controller is maintained during the identification experiment.

The results of implementing this scheme are shown in Figures 8 and 9. The changing setpoint can be seen with the pH measurement in the first subplot. The second and third subplot show the CO_2 flow and the PAR profile, respectively.

In both cases, as the pH is higher than its setpoint when the experiment starts, the first setpoint change is lower than the optimal setpoint. It can also be seen that the control signal changes abruptly when a change is made to the setpoint, and the CO_2 flow injected during the experiment is no longer square-shaped. This ensures a correct excitation of the pH regardless of the conditions, both of the culture and the weather. It should be noticed that, in this experiment, the oscillations due to the microalgae recirculation present a smaller amplitude and their attenuation is faster than the ones presented in the experiments shown in Section 3.1.1. This is mainly due to keeping the controller working while exciting the system, which is an advantage of the suggested methodology. This setup is also directly applicable to other reactors, different in shape and dimensions.

This experiment was implemented in the raceway reactor during several days, distributed along three different months, in order to tune the parameters correctly to achieve a sufficient excitation of the system without taking it far from the operating point. As it has proven to work correctly and, given the advantages it presents over the classic relay-based feedback experiment, it was chosen over the previous one in order to be implemented for control purposes.

3.2. Model identification

As mentioned in Section 2.2, the pH can be modeled as a first-order plus time delay (FOTD) transfer function with respect to CO_2 flow injection. This can be expressed as shown in Equation (2):

$$G(s) = \frac{pH(s)}{CO_2(s)} = \frac{b}{s+a} \cdot e^{-t_d s}, \tag{2}$$

where $1/a$ represents the time constant (τ) and b/a represents the static gain (k) shown in Equation (1). This representation of the transfer function was chosen given that, when the optimization process fits the model, an integrating system can also be fitted by choosing $a = 0$.

The proposed identification procedure seeks to obtain suitable model parameters while always complying with the computational cost limitation imposed by the sampling time. It begins by defining the parameter search space. Based on prior system knowledge, an array of candidate values is constructed for a, ensuring the search is conducted within a relevant range [11]. It has been seen that the time constant values may vary between 200 and 8000 seconds, but their most common values are concentrated between 500 and 2000, approximately. Therefore, the array of a candidates has been designed to contain approximately 5000 values between $1.25 \cdot 10^{-4}$ and $5 \cdot 10^{-3}$, and it also includes 0, to allow the integrator. This choice allows having a bigger concentration of elements in the range in which the time constant is usually found, while still allowing rarer values. Once this set of values is established, each candidate's system response is simulated by assuming an initial unitary gain ($b = 1$), which results in a model output (y_m). Next, the real system gain is determined by performing the left matrix division $b = y_m \backslash y$, where y represents the system output. This allows adjusting the model output by scaling it with the computed gain. This ensures the modeled response is correctly scaled to match the system's behaviour.

To evaluate each model's accuracy, a cost function J is computed to measure the difference between the adjusted model output and the real system output. A common choice for the cost function is the mean squared error (MSE), given by Equation (3),

$$J = \frac{1}{N} \sum_{i=1}^{N} \left(y(i) - y_m(i)\right)^2, \tag{3}$$

with N being the number of samples. This cost function quantifies the discrepancy between the modeled and actual outputs, providing a basis for model selection.

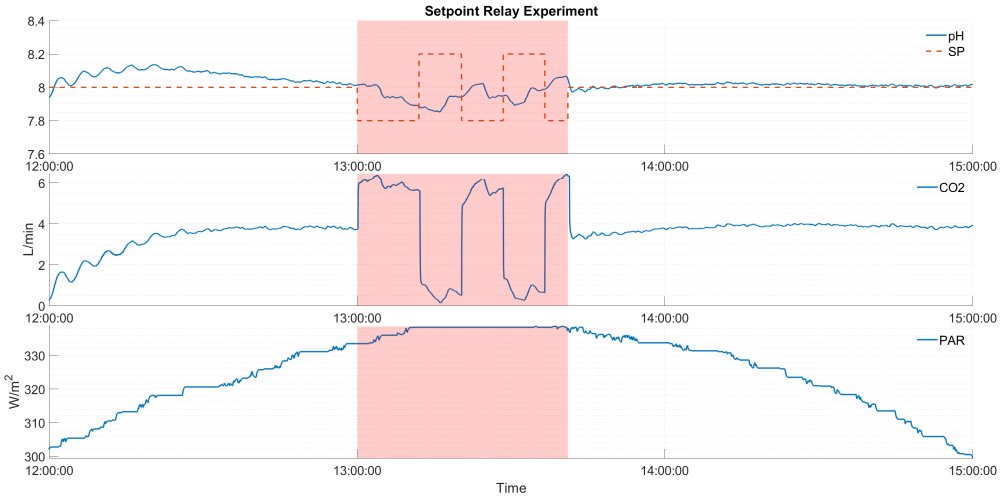

Figure 8: Setpoint relay-based autotuner results - Clear-sky day. The first subplot shows the pH response in blue and its setpoint in a red dashed line. The second and first subplots show the CO_2 flow and the PAR radiation, respectively. The area highlighted in pink represents the experiment duration.

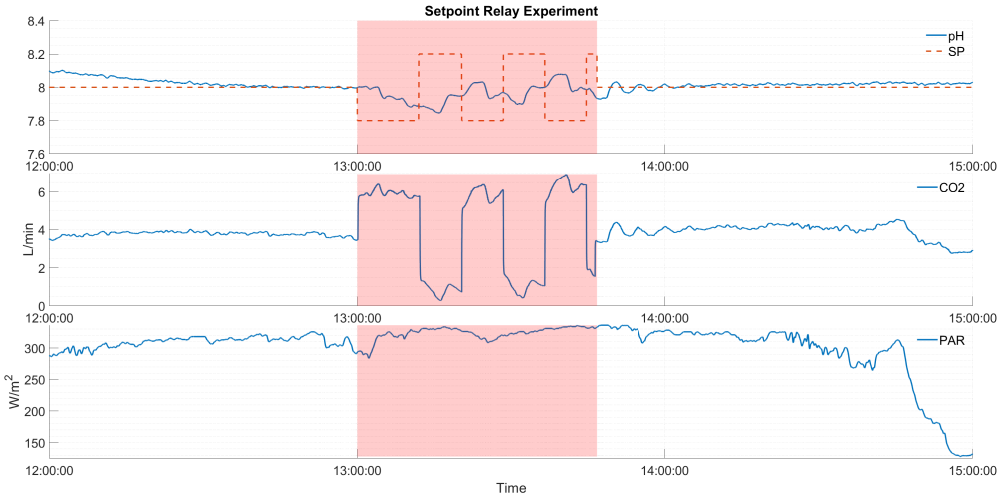

Figure 9: Setpoint relay-based autotuner results - Cloudy day. The first subplot shows the pH response in blue and its setpoint in a red dashed line. The second and first subplots show the CO_2 flow and the PAR radiation, respectively. The area highlighted in pink represents the experiment duration.

Finally, after evaluating all candidate values of a, the model corresponding to the lowest cost function value is selected as the best representation of the system. This approach systematically refines the parameter selection process, ensuring an optimal fit to the system response. The identification process is done fast enough to always be under the control sampling time, being 20 seconds.

The obtained models for the experiments shown in Section 3.1 can be seen in Figure 10. Sub-figures 10b and 10a show the identified models for the classic relay-based experiments, while Sub-figures 10d and 10c show the obtained models for the experiment where the relay is applied to the setpoint. In all four examples, the model successfully captures the main dynamic of the pH, but the model's fit is severely affected by a secondary dynamic: an oscillatory behaviour whose period is equal to the recirculation time of the culture, as explained in Section 2.2. Although there is no interest in capturing these oscillations with the model, given that they can not be controlled or eliminated, they provoke a drop in the model's fit, even after filtering them. After implementing these experiments for several weeks

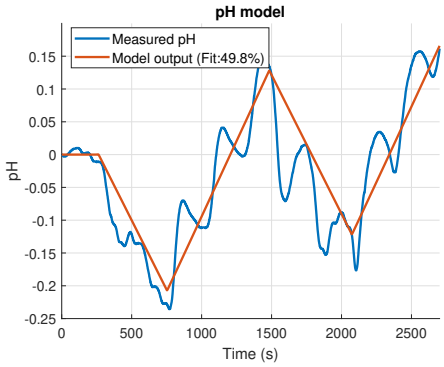

(a) Classic relay-based result - Clear day

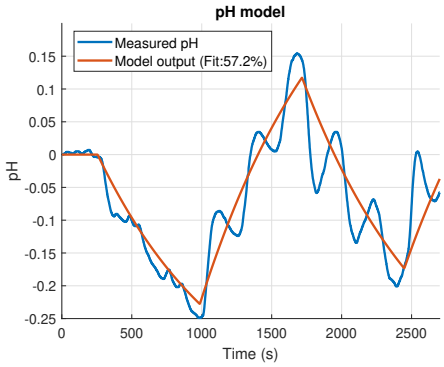

(b) Classic relay-based result - Cloudy day

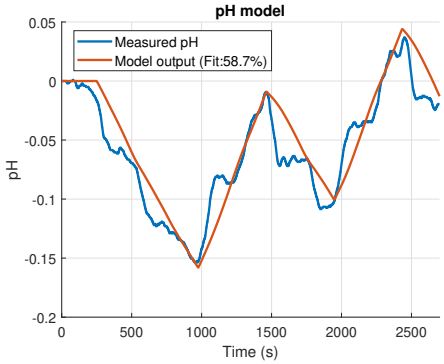

(c) Setpoint relay-based result - Clear day

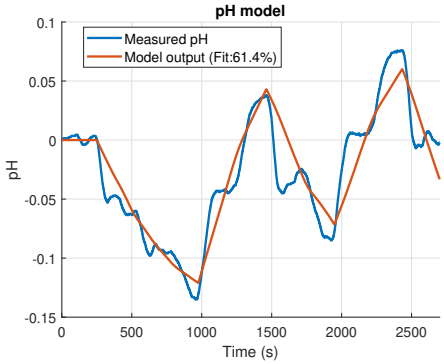

(d) Setpoint relay-based result - Cloudy day

Figure 10: Validation of the identified models for the experiments shown in Section 3.1. Figures 10a and 10b correspond to the results obtained during the classic relay-based experiments shown in Figures 5 and 6, respectively. Figures 10c and 10d correspond to the results obtained during the setpoint relay-based experiments shown in Figures 8 and 9, respectively.

and performing the identification process for almost 50 days, it has been seen that a 40% fit is good enough to represent the main dynamic, and that this low value is mainly due to these oscillations. The model's fit was calculated using Matlab's *Goodness of Fit* function with the normalized root mean squared error (NRMSE) as cost function. It can also be noticed that maintaining the closed-loop controller during the system excitation provokes a decrease in the amplitude of these oscillations, allowing a better model fit, introducing a new advantage of the proposed method. It is important to note that the pH response presents recirculation-induced oscillations, which have a period equal to the culture's recirculation time. In [9], a second-order transfer function was included to capture these oscillations. However, notice that this high-frequency dynamics is not relevant for control design purposes in accordance with the dominant dynamics captured by the FOTD and the required closed-loop system bandwidth. Thus, it can be neglected in the control design process.

Table 1 shows the parameters of each model, as well as its fit percentage, for the experiments shown in Figure 10. It can be seen that, thanks to the followed identification methodology, the pH can be modeled as a first-order plus time delay or as an integrator plus time delay. This will exclusively depend on the cost function defined in Equation (3), prioritizing the model's fit percentage. It is important to remark that, in presence of CO_2 injection, the system can be modeled as a first order, while in its absence it presents an exponential growth. Also, the first-order time constant can present large values with respect to the time delay, in which cases it may be convenient to represent the system with an integrator.

Once the experiment has proven to obtain an appropriate pH's dynamic that allows the obtention of a model, it is necessary to establish an automatic way to determine the goodness of the experiment. The model must be discarded if one of the following happens: the model's fit is not good enough, the model's parameters are not appropriate, or there are strong disturbances during the experiment that can affect the model's parame-

Experiment	a	b	k	τ	Fit (%)
Classic relay - Cloudy day	0.0011	-2.217E-04	-0.2099	946.9	57.2
Classic relay - Clear day	0	-2.215E-04	-	-	49.8
Setpoint relay - Cloudy day	0.0015	-1.124E-04	-0.0757	673.8	61.4
Setpoint relay - Clear day	0	-9.861E-05	-	-	58.7

Table 1: Models' parameters and fit percentage for experiments in Figure 10.

ters.

3.3. Goodness of the experiment

After the experiment is finished and the parameters are estimated, a decision must be made on retuning the PI controller.

The model's FIT and the parameters' values are analysed to evaluate the model's validity. First, b must be negative, given that an increase in CO_2 flow injection will provoke a decrease in pH. On the other hand, a can have any value from the defined search space. Lastly, the model's fit must be above 40% to ensure good system representation.

Apart from the model analysis, disturbances during the experiment must be considered. Significant disturbances entering the system during the relay experiment can create problems, such as stopping the process from oscillating as expected and not obtaining proper excitation of it [24].

As mentioned in Section 2.2, the main disturbances affecting pH are the dilution and the solar radiation. In this work, two strategies are followed to ensure there are no disturbances during the experiment. Given that dilution is an operational process that can be manipulated, this is annulled during the 45 minutes of the experiment, and its operation returns to normal once it is finished.

Radiation, however, can not be manipulated. Therefore, once the experiment is finished, days with passing clouds must be detected to reject those experiments in the adaptation procedure. For this purpose, the PAR is analysed and the period is classified as "cloudy" or "clear" using a *Fine Tree* model trained with the *Classification Learner Toolbox* from Matlab. The model uses as features the difference between the maximum and minimum values,

$$\Delta PAR = max(PAR) - min(PAR), \tag{4}$$

and the integral of the noise in the PAR signal. For this last feature, the radiation is previously filtered with a high-pass filter to eliminate the slow trend and maintain the high frequency of passing clouds. After, the integral of the absolute value must be applied to the filtered signal, calculated as follows,

$$\begin{aligned} PAR_F(i) =& PAR(i) - PAR(i-1) + \\ & (1 - \alpha \cdot T_s) \cdot PAR_F(i-1), \end{aligned} \tag{5}$$

where PAR is the measured value of PAR, PAR_F is its filtered value, i is the discrete time instant, T_s is the sample time, and α is the filter cut-off frequency, which has been established by testing the filter on a clear-sky radiation profile. The filtered radiation PAR_F is integrated during the period of the experiment, obtaining

$$Int_{PAR_F} = \sum_{i=1}^{N} PAR_F(i), \tag{6}$$

where $i = 1$ and $i = N$ are the initial and final time samples of the experiment, and $PAR_F(i)$ is the filtered value of the radiation in the sample time i.

In Figure 11, two examples of this process can be seen. The superior row shows the results of filtering a clear sky time period, while the inferior row shows a PAR profile typical of a cloudy day. The graph on the left shows the complete day data, the middle one shows the irradiance during the period in which the experiment is done, and the graph on the right shows the result of filtering the PAR. A clear difference can be observed between filtered radiation on a clear day and on a cloudy day.

After calculating ΔPAR and Int_{PAR_F}, and manually classifying the intervals of a total of 98 days in similar seasons, a *Fine Tree* was trained using the *Classification Learner Toolbox* from *Matlab*, obtaining a 98.9% of accuracy when a prediction is made. The model uses both parameters as features to predict the presence of passing clouds. The training data can be observed in the scatter plot shown in Figure 12, where a clear difference between both types of day can be easily observed. Notice that although this model presented promising results and worked perfectly in the experiments performed in this work, the dataset should be periodically updated with more data to make it more robust.

Thus, once the model's parameters and FIT have been validated and the PAR profile has been classified as a clear day using the model described above, the algorithm proceeds with the PI controller retuning.

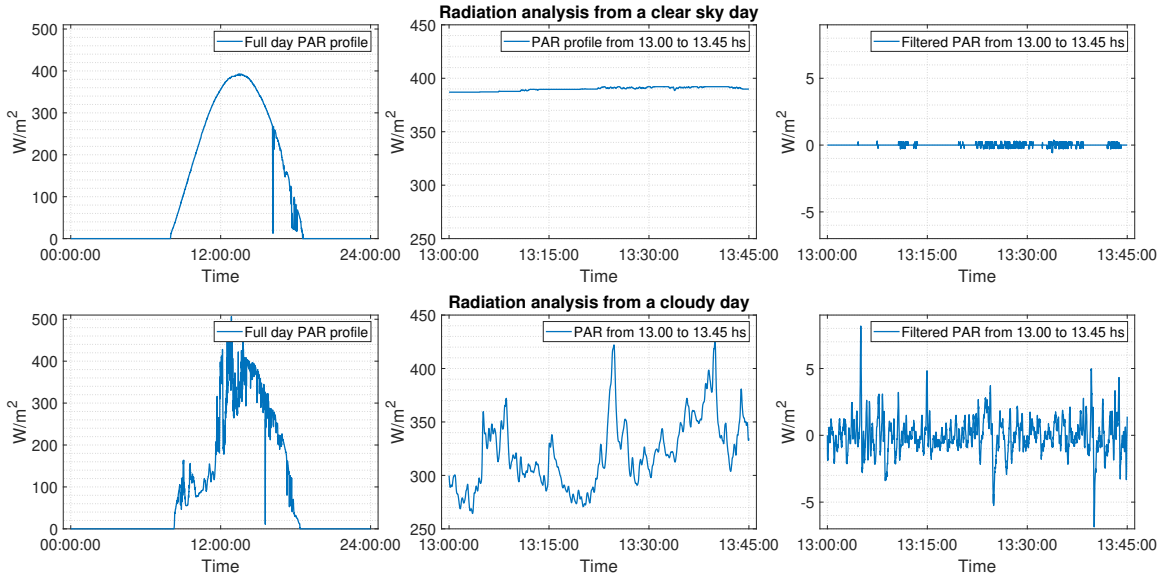

Figure 11: High-pass filtered PAR in clear and cloudy days. The first row shows the results for a clear-sky day, while the second shows a day with passing clouds. For each day, the right picture shows the complete PAR profile, the middle plot shows the PAR during the experiment, and the figure on the right shows the filtered PAR.

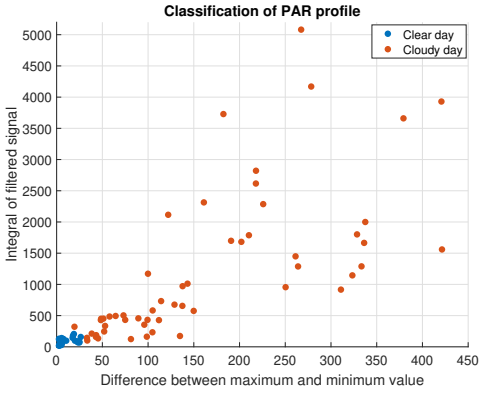

Figure 12: Classification model training data, where the vertical axis represents the integral of the filtered PAR (Int_{PAR_F}) and the horizontal axis represents the difference between the maximum and minimum value (ΔPAR). Cloudy days are represented with orange dots, while blue dots represent clear-sky profiles.

3.4. Controller tuning method

A PI controller was selected over a PID structure due to the dominant FOTD behavior observed in the process. The absence of significant oscillatory dynamics in the pH response, combined with the presence of high-frequency noise, makes derivative action unnecessary and potentially counterproductive. Therefore, a PI controller was deemed sufficient to achieve stable regulation, in line with established industrial practices and recommendations such as those found in [25]. The controller, which is of the form shown in Equation (7), was tuned using the SIMC rules, developed in [25].

$$C(s) = K_p\left(1 + \frac{1}{T_i \cdot s}\right), \tag{7}$$

where K_p is the proportional gain, and T_i is the integral time constant. Due to the form of the system identified (Equation (2)), the model can turn into a first order (FOTD) or an integrator (ITD), both with time delay.

Therefore, the PI parameters are tuned, depending on the form of the model, following the equations shown in Table 2, where τ_{cl} is the closed-loop time constant, chosen equal to the time delay, t_d, following the recommendations in [25].

	FOTD	**ITD**
K_p	$\frac{1}{k} \cdot \frac{\tau + t_d/3}{\tau_{cl} + t_d}$	$\frac{1}{b} \cdot \frac{1}{\tau_{cl} + t_d}$
T_i	$min\{\tau + t_d/3, 4 \cdot (\tau_{cl} + t_d)\}$	$4 \cdot (\tau_{cl} + t_d)$

Table 2: PI parameters tuning equations

The PI controller also includes back-calculation anti-windup, one of the most common anti-windup methods, where the integrating term is dynamically changed with

a tracking time constant (T_t) when the control signal saturates [26]. There are several suggestions to tune the tracking time constant in the literature, but, in general, it is recommended to set it in the interval $0 \leq T_t \leq T_i$. However, if the tracking time is set too small ($T_t << T_i$), it may cause an extremely fast resetting of the controller, provoking a saturation at the upper limit and a severe performance deterioration [27]. In this work, the tracking time was established equal to the integrating time constant ($T_t = T_i$).

Lastly, a static feedforward compensator (FF) is added so as counteract solar radiation disturbances on pH. The feedforward gain (K_{FF}) is obtained as the ratio between the static gains of the controlled variable in relation to the control signal (P_u) and the load disturbance (P_d), which in this case is the PAR radiation. This means that

$$FF = K_{FF} = \frac{K_d}{K_u}, \tag{8}$$

where K_d and K_u are the static gains of the disturbance and the control signal transfer functions, respectively. Despite its easy tuning methodology, this feedforward compensator provides a significant improvement in the disturbance rejection. To tune this gain, the procedure suggested in [28] was followed, by observing the required change in the control signal when there is a change in the disturbance, once the controlled variable is in the fixed setpoint and the control loop is in steady state.

Adding up the different structures, the final controller structure is shown in Figure 13, where PI represents the Proportional-Integral controller plus antiwindup strategy and FF represents the static feedforward. During regular operation, the reference is established at the optimal pH value, equal to 8. When an experiment is to be performed, a ±0.2 relay signal is added to the original setpoint during 45 minutes. Once the experiment is done, the model is identified, the validity of the data is analysed, and the controller's parameters are retuned, if necessary.

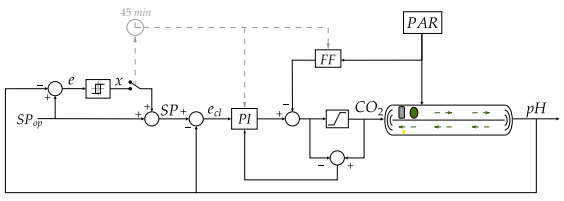

Figure 13: Final controller diagram. The full control structure includes the PI controller, the static feedforward for radiation compensation, and antiwindup. When the identification experiment is performed, the relay signal is added to the setpoint.

4. Results

After designing the experiment and proving the system's excitation is enough to obtain an accurate model, the structure shown in Figure 13 was implemented in one of the reactors available at the IFAPA research center, explained in Section 2.1. In parallel, in the second reactor, a fixed PI controller with static feedforward was implemented. This controller was tuned using a nominal model that is good enough to represent the pH's dynamics through various conditions [11]. The model is the one shown in Equation (9) and, by using the tuning rules described in Section 3.4, the controller results as shown in Equation (10).

$$G(s) = \frac{pH(s)}{CO_2(s)} = \frac{-0.18}{1100s + 1} \cdot e^{-300s}. \tag{9}$$

$$C(s) = -11.11\left(1 + \frac{1}{1200s}\right). \tag{10}$$

The static feedforward was designed as described in Section 3.4, resulting in

$$K_{FF} = \frac{K_d}{K_u} = -0.01\ (m^2 \cdot L)/(W \cdot min), \tag{11}$$

with $K_u = -0.18$ min/L and $K_d = 0.0018$ m^2/W, calculated based on previous experiments. Then, when a new model is fitted, the static feedforward can be retuned by calculating the ratio between the new process gain, K_u, and the fixed disturbance gain, K_d. Notice that although K_d can slightly change along the seasons, the more relevant contribution to the feedforward action comes from the variation in K_u. For this reason, it was decided to keep K_d constant along the experiments.

The implementation of both strategies began with the same parameters in both the adaptive and the fixed controller, in order to make a fair comparison between them. Each day, at 13.00 p.m., the experiment is performed and, if the conditions explained in Section 3 are met, the controller's parameters are retuned.

The results of implementing both strategies for five consecutive days are shown in Figure 14. The first subplot shows the pH obtained by both, the fixed (in blue) and the adaptive (in red), control strategies, as well as the setpoint for the adaptive controller, which includes the relay changes when the identification experiment is performed, between 1.00 and 1.45 p.m. The pink shadowed region represents the period corresponding to the relay-based experiment. The second subplot shows the CO_2 flow injected by each strategy, while the third subplot shows the dilution pulses corresponding to each reactor. Lastly, the fourth subplot shows the PAR for each day.

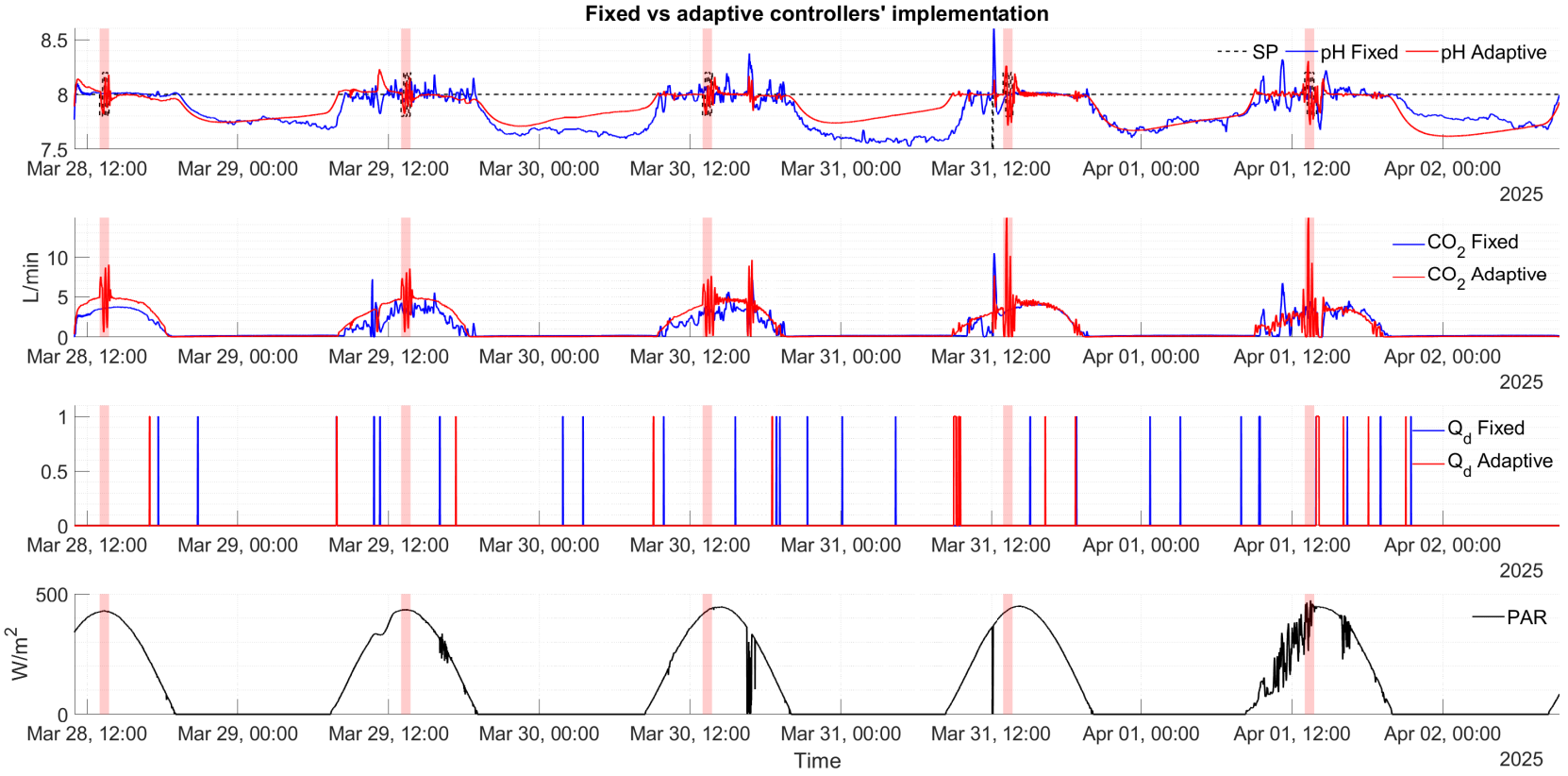

Figure 14: Results of implementing fixed (in blue) and adaptive (in red) PI controllers. The first subplot shows the pH measurement and the setpoint (in dashed black), and the second shows the control signal (CO_2 flow). The third and fourth subplots show the most important disturbances, dilution and radiation, respectively. The areas highlighted in light pink represent the period in which the experiment is performed.

Each day, the controllers start running when the PAR is higher than 20 W/m^2 and the pH's value reaches the setpoint. As explained previously, on the first day, both controllers start running with the same parameters' values. The adaptive controller is updated every day after the experiment, except for the last day, when the model's fit is not good enough, and there is a strong presence of passing clouds. The obtained models can be seen in Figure 15, where they are compared with the measured pH.

During the first day, it can be seen that the fixed PI controller is able to maintain pH close to the setpoint during the entire day and presents a better behaviour than the adaptive strategy. After the experiment, the controller is updated, and its performance seems to improve, but a dilution pulse at around 5.00 p.m. slightly drops the pH, taking it away from the operating point. On the second day, the fixed controller presents an aggressive behaviour, resulting in a noisy measurement of the pH, while the adaptive controller obtains a smoother dynamic. An important aspect to mention is that, between 11.00 a.m. and 12.20 p.m., there is a sudden change in the irradiance, to which the adaptive controller reacts aggressively, provoking a quick rise in pH. In the reactor with the fixed controller, this change in the irradiance happens simultaneously with two dilution pulses that cause the contrary effect, a sudden drop in pH. Both controllers are able to get pH back to the setpoint after a short period. During the third day, the behaviour obtained by the designed strategy is also better than the classical approach, obtaining a better pH regulation and maintaining it closer to the setpoint. The controller is once more tuned after the experiment is performed, as the model's fit is over 50%, and there is no presence of passing clouds. A strong disturbance can be seen at around 5.00 p.m., where radiation drops abruptly to almost zero. In this case, the CO_2 injected by the adaptive controller presents a more aggressive behaviour attributed to the adaptation of the feedforward gain, allowing a much quicker rejection of the disturbance and maintaining pH closer to the operating point than the fixed controller. On the fourth day, a sudden change in the pH and the CO_2 flow can be observed at noon, due to a communication loss with both controllers. This provoked an increase in pH in both reactors, which the adaptive controller could control faster, taking the controlled variable back to the setpoint faster than the fixed PI. Finally, the last day presents a cloudy profile in the irradiance, and both controllers present a noisy behaviour, although the adaptive one is able to reject the clouds more efficiently. In this case, as the model's fit is not good enough (less than 30%), and there are passing clouds during the experiment, the parameters were not changed, and the ones obtained in the previous day were maintained.

Apart from obtaining a better pH regulation during the day, the adaptive strategy is able to keep the pH closer to the setpoint during the night in almost every case. This is particularly important for the microalgae activity during the daily period, as they perform better and with less stress if pH is close to 8 at sunrise. Although the adaptive controller generally injects more CO_2 during the day, this is done efficiently and with small pH oscillations, allowing the microalgae to absorb all the carbon from the medium during the light hours and perform photosynthesis with it. In this way, there is less accumulated carbon in the medium at sunset, and the pH drop during the night is much lower than in the case of the classical controller. This can be especially appreciated during the second and third nights, where the pH of the fixed strategy decreases more than that of the adaptive controller. During the last night, although the adaptive strategy presents a more abrupt decrease in pH, it exhibits a much faster recovery as soon as solar radiation is available, reaching the operating point practically simultaneously with the fixed strategy at sunrise.

Regarding the dilution pulses, these occur at different times for each reactor, depending on the measured level in each case. However, their effect is not too strong, and has the form of little peaks, as can be seen especially during the second and third nights in the fixed strategy pH (Figure 14). It must also be reminded that dilution is either a planned operation or a response from the automated system to level measurement but, in any case, this can be manipulated without further consequences. In future works, the operation could be enhanced by taking dilution's effect into account in the control loop.

Figure 15 shows the models obtained each day. It can be seen that, except for the last day, a very good fit is obtained. Table 3 shows the parameters for each model and the resulting controller. For each day, the parameters of the fitted model (a, b, K, and τ) can be observed, as well as the goodness of fit in each case. It can be seen that the fit is always above 50%, except for the last day. Therefore, the first four days, the controller is adapted with the parameters K_p, T_i, T_t, and K_{FF} shown in the Table, while the last day maintains the previous ones. In the first row of the table, the initial parameters can be seen, which are the same as the ones used in the fixed controller. Notice that high variability of the process parameters in consecutive days, which confirms the necessity of adaptive controllers to account for this control problem. pH dynamics is affected by multiple phenomena, such as biomass concentration, culture depth, total

inorganic carbon, dilution rate, nutrient concentrations, etc., which make the dynamics really changing.

Apart from the benefits that can be seen graphically from Figure 14, metrics such as the IAE (Integral Absolute Error), ISE (Integral Square Error), ITAE (Integral of Time multiplied Absolute Error), ITSE (Integral of Time multiplied Square Error), Control Effort (the variation in the control signal), and CO_2 consumption were calculated to compare both performances numerically.

As a result, the adaptive strategy improved the metrics related to the error: it obtained a reduction in the IAE and the ISE of 12 and 7%, respectively. The ITAE and ITSE obtained by the autotuner were 48 and 68% smaller than the ones obtained by the classical approach. Finally, although the CO_2 consumption was increased by 20%, the control effort was lowered by 10% with respect to the fixed controller. Therefore, the results prove a better performance of the designed methodology for autotuning a simple controller, both graphically and quantitatively.

5. Discussion

This paper presents an adaptive autotuning strategy for pH control in microalgae raceway reactors, based on relay-based autotuners principles. The approach is specifically designed to handle the daily and seasonally varying dynamics of the culture systems. Two relay self-tuning schemes were explored and experimentally validated: a classical approach with controller disconnection and a novel setpoint relay method. Although successful in exciting the system, the classical approach could require manual recalibration to adapt to seasonal changes or different reactor configurations. In contrast, the setpoint relay method operates with the PI controller in a closed loop, applying the relay signal to the setpoint. This approach allows seamless integration into existing control loops without the need for manual recalibration across seasons or for different reactors. Experimental validation showed that this method excites the system adequately, producing appropriate dynamic responses for model identification.

The adaptive strategy couples a Proportional-Integral (PI) controller, tuned using SIMC rules, with a static feedforward compensation to counteract solar radiation disturbances. Model identification is based on first-order or integrator structures with delay, selecting the model that best fits the experimental data by minimizing the mean square error.

Model validation and disturbance handling measures were implemented to ensure the reliability of the autotuning. The model's validity is assessed by analysing the fit percentage and parameter values. Disturbances, such as dilution, were cancelled out during the experiment. For the solar radiation, a classification algorithm was introduced to evaluate the presence of passing clouds by analysing its profile. Data from experiments performed under strong disturbances or with a poor model fit are discarded for retuning.

The adaptive control strategy was validated in an industrial-scale raceway reactor for five consecutive days and compared to a fixed PI controller. The results showed that the adaptive controller outperformed the fixed controller most days, achieving a smoother pH regulation closer to the setpoint. It could reject disturbances such as abrupt changes in solar radiation or communication losses quicker and more efficiently. In addition, the adaptive strategy resulted in less carbon accumulated at the end of the day, leading to a lower pH drop during the night compared to the fixed controller. As a result of the enhanced pH control, not only is culture stability ensured and biomass production maximized, but also availability of inorganic carbon is guaranteed and the growth of the desired strain promoted, helping mitigate biological risks such as contamination by fungal predators and nitrogen accumulation. It must also be taken into account that this algorithm allows an easy adaptation of the models and the controller throughout the entire year.

6. Conclusions

In conclusion, this work presents and experimentally validates an adaptive relay-based autotuning strategy, highlighting the superiority of the novel set-point relay method for pH regulation in microalgae reactors. The strategy provides a reliable, scalable, and low-intervention solution for adaptive pH control, demonstrating reliable performance in variable weather conditions and improving culture productivity by maintaining pH within the optimal range more effectively.

Acknowledgments

This work has been financed by the following projects: the European Union under the agreement of grant no. 101060991 REALM and the project no. PID2023-150739OB-I00 financed by the Spanish Ministry of Science. Malena Caparroz acknowledges the financial support of the Spanish Ministry of Science, Innovation, and Universities under grant FPU23/02235. The Lund Univesity co-authors are members of the ELLIIT strategic research area. The authors also acknowledge the Erasmus grant given by ceiA3 that allowed her

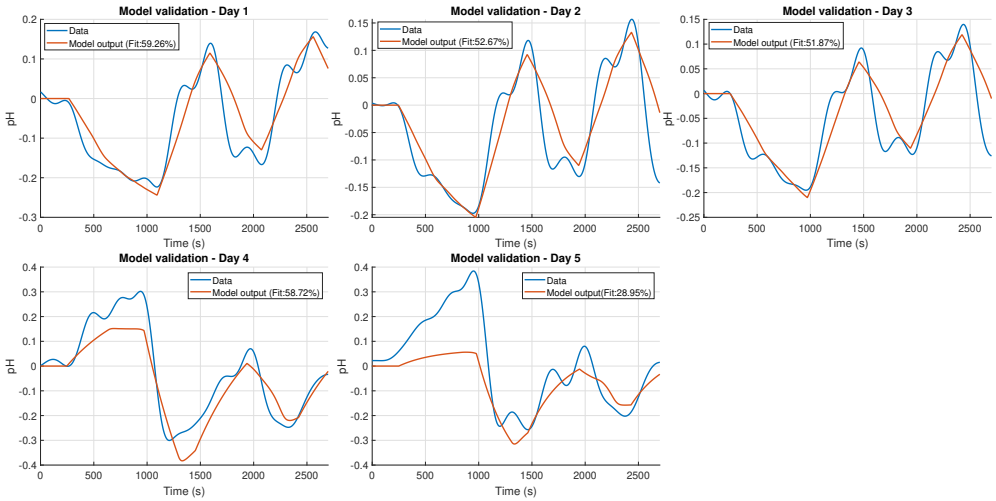

Figure 15: Models' fit during implementation of the adaptive controller (Figure 14). The pH measurement is shown in blue, while the model output is represented in red.

Day	a	b	K	τ	FIT (%)	Parameters retuning	K_p	T_i,T_t	K_{FF}
	-	-	-	-	-	-	-11	1100	0.01
1	0.0002	-1.91E-04	-0.8744	4587	59.26	Yes	-8.93	2400	0.0021
2	0.0004	-1.67E-04	-0.3794	2267	52.67	Yes	-10.40	2367	0.0047
3	0.0001	-1.55E-04	-1.2396	8000	51.87	Yes	-10.89	2400	0.0015
4	0.0016	-1.52E-04	-0.0966	633	58.72	Yes	-12.66	733	0.0186
5	0.003	-1.17E-04	-0.0392	335	28.95	No	-12.66	733	0.0186

Table 3: Model and controller parameters for the results shown in Figure 14.

research stay in Lund, allowing the collaboration between both institutions.

References

[1] S. A. Razzak, K. Bahar, K. O. Islam, A. K. Haniffa, M. O. Faruque, S. Z. Hossain, M. M. Hossain, Microalgae cultivation in photobioreactors: Sustainable solutions for a greener future, Green Chemical Engineering 5 (4) (2024) 418–439, https://doi.org/10.1016/j.gce.2023.10.004.

[2] B. S. Yu, S. Pyo, J. Lee, K. Han, Microalgae: a multifaceted catalyst for sustainable solutions in renewable energy, food security, and environmental management, Microbial Cell Factories 23 (1) (2024) 308, https://doi.org/10.1186/s12934-024-02588-7.

[3] N. Hossain, T. Mahlia, R. Saidur, Latest development in microalgae-biofuel production with nano-additives, Biotechnology for Biofuels 12 (2019) 1–16, https://doi.org/10.1186/s13068-019-1465-0.

[4] P. Darvehei, P. A. Bahri, N. R. Moheimani, Model development for the growth of microalgae: A review, Renewable and Sustainable Energy Reviews 97 (2018) 233–258, https://doi.org/10.1016/j.rser.2018.08.027.

[5] G. Zuccaro, A. Yousuf, A. Pollio, J.-P. Steyer, Chapter 2 - microalgae cultivation systems, in: A. Yousuf (Ed.), Microalgae Cultivation for Biofuels Production, Academic Press, 2020, pp. 11–29, https://doi.org/10.1016/B978-0-12-817536-1.00002-3.

[6] R. Nordio, E. Viviano, A. Sánchez-Zurano, J. G. Hernández, E. Rodríguez-Miranda, J. L. Guzmán, G. Acién, Influence of pH and dissolved oxygen control strategies on the performance of pilot-scale microalgae raceways using fertilizer or wastewater as the nutrient source, Journal of Environmental Management 345 (2023) 118899, https://doi.org/10.1016/j.jenvman.2023.118899.

[7] R. Nordio, S. Belachqer-El Attar, E. Clagnan, A. Sánchez-Zurano, N. Pichel, E. Viviano, F. Adani, J. L. Guzmán, G. Acién, Exploring microbial growth dynamics in a pilot-scale microalgae raceway fed with urban wastewater: Insights into the effect of operational variables, Journal of Environmental Management 369 (2024) 122385, https://doi.org/10.1016/j.jenvman.2024.122385.

[8] J. Masojídek, K. Ranglová, G. E. Lakatos, A. M. Silva Benavides, G. Torzillo, Variables governing photosynthesis and growth in microalgae mass cultures, Processes 9 (5) (2021) 820, https://doi.org/10.3390/pr9050820.

[9] M. Berenguel, F. Rodríguez, F. G. Acién, J. L. García, Model predictive control of pH in tubular photobioreactors, Journal of Process Control 14 (4) (2004) 377–387, https://doi.org/10.1016/j.jprocont.2003.07.001.

[10] R. Nordio, E. Rodríguez-Miranda, F. Casagli, A. Sánchez-Zurano, J. L. Guzmán, G. Acién, Abaco-2: a comprehensive model for microalgae-bacteria consortia validated outdoor at pilot-scale, Water Research 248 (2024) 120837, https://doi.org/10.1016/j.watres.2023.120837.

[11] M. Caparroz, J. L. Guzmán, M. Berenguel, F. G. Acién, A novel

data-driven model for prediction and adaptive control of pH in raceway reactor for microalgae cultivation, New Biotechnology 82 (2024) 1–13, https://doi.org/10.1016/j.nbt.2024.04.001.

[12] P. Otálora, J. L. Guzmán, M. Berenguel, F. G. Acién, Data-driven pH model in raceway reactors for freshwater and wastewater cultures, Mathematics 11 (7) (2023) 1614, https://doi.org/10.3390/math11071614.

[13] F. R. Rubio, M. J. López Sánchez, Control Adaptativo y Robusto, Universidad de Sevilla, 1996, ISBN: 978-84-472-0319-2.

[14] M. Caparroz, J. L. Guzmán, J. D. Gil, M. Berenguel, F. G. Acién, A hybrid MRAC-PI approach to regulate pH in raceway reactors for microalgae production, Control Engineering Practice 156 (2025) 106191, https://doi.org/10.1016/j.conengprac.2024.106191.

[15] K. J. Åström, T. Hägglund, Automatic tuning of simple regulators with specifications on phase and amplitude margins, Automatica 20 (5) (1984) 645–651, https://doi.org/10.1016/0005-1098(84)90014-1.

[16] J. González-Hernández, E. Rodríguez-Miranda, J. L. Guzmán, F. G. Acién, A. Visioli, Temperature optimization in microalgae raceway reactors by depth regulation, Revista Iberoamericana de Automática e Informática Industrial 19(2) (2022) 164–173, https://doi.org/10.4995/riai.2022.16586.

[17] M. Barceló-Villalobos, C. G. Serrano, A. S. Zurano, L. A. García, S. E. Maldonado, J. Peña, F. A. Fernández, Variations of culture parameters in a pilot-scale thin-layer reactor and their influence on the performance of Scenedesmus Almeriensis culture, Bioresource Technology Reports 6 (2019) 190–197, https://doi.org/10.1016/j.biteb.2019.03.007.

[18] E. Rodríguez-Miranda, J. L. Guzmán, M. Berenguel, F. G. Acién, A. Visioli, Diurnal and nocturnal pH control in microalgae raceway reactors by combining classical and event-based control approaches, Water Science and Technology 82 (6) (2020) 1155–1165, https://doi.org/10.2166/wst.2020.260.

[19] K. J. Åström, T. Hägglund, Practical experiences of adaptive techniques, in: 1990 American Control Conference, IEEE, 1990, pp. 1599–1606, https://doi.org/10.23919/ACC.1990.4791005.

[20] T. Hägglund, K. J. Åström, Industrial adaptive controllers based on frequency response techniques, Automatica 27 (4) (1991) 599–609, https://doi.org/10.1016/0005-1098(91)90052-4.

[21] J. Berner, T. Hägglund, K. J. Åström, Asymmetric relay autotuning–practical features for industrial use, Control Engineering Practice 54 (2016) 231–245, https://doi.org/10.1016/j.conengprac.2016.05.017.

[22] C. C. Hang, K. J. Åström, Q. G. Wang, Relay feedback auto-tuning of process controllers—a tutorial review, Journal of Process Control 12 (1) (2002) 143–162, https://doi.org/10.1016/S0959-1524(01)00025-7.

[23] T. Hägglund, K. J. Åström, An industrial adaptive PID controller, IFAC Proceedings Volumes 23 (1) (1990) 251–256, https://doi.org/10.1016/S1474-6670(17)52729-9.

[24] J. Berner, Automatic controller tuning using relay-based model identification, Doctoral thesis (compilation), Department of Automatic Control, Lund Institute of Technology, Lund University (2017).

[25] S. Skogestad, C. Grimholt, The SIMC Method for Smooth PID Controller Tuning, in: Vilanova, R., Visioli, A. (eds) PID Control in the Third Millennium. Advances in Industrial Control. Springer, London, 2012, https://doi.org/10.1007/978-1-4471-2425-2_5.

[26] K. J. Åström, T. Hägglund, Advanced PID control, ISA-The Instrumentation, Systems and Automation Society, 2006.

[27] L. Rundqwist, Anti-reset windup for PID controllers, IFAC Proceedings Volumes 23 (8) (1990) 453–458, https://doi.org/10.1016/S1474-6670(17)51865-0.

[28] J. L. Guzmán, T. Hägglund, Feedforward Control: Analysis, Design, Tuning rules, and Implementation, Walter de Gruyter GmbH & Co KG, 2024.